

ABSTRACT

CHEMISTRY

DIAS, BENJAMIN

B.S., Inter American University, 1969

Antiferromagnetic Coupling Constants for Some Iron Porphyrin μ -Oxo-Dimers.

Adviser: Dr. G. Scott Owen

Thesis dated August 1, 1975

Many studies have been performed on the antiferromagnetic interaction in $\text{Fe}^{\text{III}}\text{-O-Fe}^{\text{III}}$ type dimers. This paper reports a study on two such porphyrin systems μ -xO-bis-(tetraphenylporphyrinatoiron (III)) and μ -OXO-bis (octaethylporphyrinatoiron (III)). In addition, we are reporting the results of a similar study on the first oxidation products of the above porphyrin μ -oxo dimers. This is the first such study of the antiferromagnetic interaction in an $\text{Fe}^{\text{IV}}\text{-O-Fe}^{\text{III}}$ type system. To obtain the singly oxidized products a constant potential electrolysis system was used. A Varian A-60 NMR spectrometer equipped with a variable temperature apparatus was used to look at the temperature dependent on the magnetic susceptibility. A non-linear least squares computer program was used to evaluate the antiferromagnetic coupling constant, J. The resulting J values indicate a greater overlap of the $\text{Fe}^{\text{III}}\text{-O-Fe}^{\text{III}}$ orbitals for the tetraphenylporphyrin μ -Oxo dimer (TPP) ($J = -344 \text{ cm}^{-1}$) than for the octaethylporphyrin μ -oxo dimer (OEP) ($J = -280 \text{ cm}^{-1}$). For both oxidized species the $\text{Fe}^{\text{IV}}\text{-O-Fe}^{\text{III}}$ orbital overlap is decreased ($J = -154 \text{ cm}^{-1}$ for the TPP μ -OXO-dimer and $J = -73 \text{ cm}^{-1}$ for the OEP μ -Oxo dimer), probably because the $\text{Fe}^{\text{IV}}\text{-O}$ bond distance is increased as the Fe^{IV} moves into the plane of the porphyrin.

DETERMINATION OF THE ANTIFERROMAGNETIC
COUPLING CONSTANTS OF SOME IRON PORPHYRIN
U-OXO-DIMERS

A THESIS
SUBMITTED TO THE FACULTY OF ATLANTA UNIVERSITY
IN PARTIAL FULFILMENT OF THE REQUIREMENTS
FOR THE DEGREE OF MASTER OF SCIENCE

BY
BENJAMIN DIAS

DEPARTMENT OF CHEMISTRY

ATLANTA, GEORGIA

MAY 1975

R =

V

T = 39

ACKNOWLEDGEMENTS

My profound gratitude goes to my adviser - Dr. C. Scott Owen who has been patient, and under whose direction I have found research to be a delightful and a rewarding experience. I am grateful to the Atlanta University Chemistry Department and other sources from which I have received financial support during the course of my studies.

I should also like to thank individual faculty and staff members whose assistance I might have relied on somewhere along the way.

I am not unmindful of fellow students, particularly Joseph Kwabbi, with whom I have had meaningful association. Finally, I should like to thank my family, who have been patient and kind.

TABLE OF CONTENTS

	Page
ACKNOWLEDGEMENTS.....	ii
LIST OF TABLES.....	iv
LIST OF FIGURES.....	v
INTRODUCTION.....	1
BACKGROUND & THEORY.....	3
EXPERIMENTAL.....	18
RESULTS & DISCUSSION.....	29
BIBLIOGRAPHY.....	38

LIST OF TABLES

Table	Page
1. Extinction coefficients for $(\text{FeTPP})_2\text{O}$, $(\text{FeTPP})_2\text{O}^+$, $(\text{FeOEP})_2\text{O}$ and $(\text{FeOEP})_2\text{O}^+$	21
2. Knight Shift Measurements of Pyrrole Protons for Neutral Species.....	30
3. Experimental results for $(\text{FeTPP})_2\text{O}$	32
4. Experimental results for $(\text{FeTPP})_2\text{O}^+$	34
5. Experimental results for $(\text{FeOEP})_2\text{O}$	35
6. Experimental results for $(\text{FeOEP})_2\text{O}^+$	36
7. Summary of results for Neutral and Oxidized Species.....	37

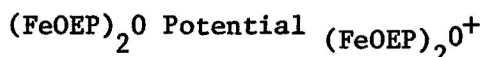
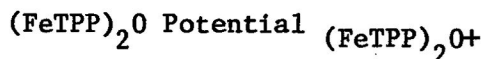
LIST OF FIGURES

Figure	Page
1. ^{III} Fe Protoporphyrin.....	3
2. Porphin.....	4
3. Hemin.....	6
4. Structure of μ -oxo-bis (porphyriniron (III)) dimer.....	6
5. Position of metal relative to pyrrole nitrogen.....	7
6. Curie-Weiss Law Plot.....	8
7. Plot of X <u>vs</u> T for Paramagnetic ion.....	9
8. d-orbital overlap.....	10
9. σ and π exchange coupling overlap.....	11
10. X vs T for antiferromagnetic compound.....	12
11. The d-orbitals.....	13
12. Electrolysis Aparatus.....	19
13. Optical Spectrum of Neutral and Oxidized TPP.....	22
14. Optical Spectrum of Neutral and Oxidized OEP.....	23
15. NMR Spectrum of Splitting of Solvent Peak.....	26
16. Graph Showing Density Correction for Solvent.....	28

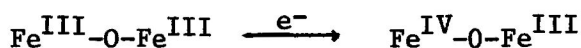
INTRODUCTION

Many compounds of the transition elements are paramagnetic, and as such much of our understanding of transition metal chemistry has been derived from magnetic data. Paramagnetism is caused by the presence in the substance of ions, atoms or molecules which have unpaired electrons. There are also more complex forms of magnetic behaviour, one of which is antiferromagnetism. This form of magnetism is a result of coupling between spins of neighbouring paramagnetic species.

Antiferromagnetism is a widespread phenomenon occurring both in inorganic metal complexes and in biological systems. Its study has been extensive, but limited to the "normal" oxidation states of the transition metals involved.¹ It is therefore, the purpose of this investigation to look at the antiferromagnetism of some well-known biological model systems with a view to evaluating their antiferromagnetic coupling constants. This will encompass, as a consequence, a study of both the neutral and singly oxidized species of at least two interesting compounds—the μ -Oxo-bis (tetraphenylporphyrinatoiron (III)), $(\text{FeTPP})_2\text{O}$, and the μ -Oxo-bis (octaethylporphyrinatoiron (III)) $(\text{FeOEP})_2\text{O}$, dimers. These reactions are best characterized as:



with the neutral and singly oxidized species represented as follows:



Some of this work has been previously attempted,³ but the results seem to indicate that further investigation would indeed prove useful.

Preference for the study of antiferromagnetism has been given to transition metal complexes, because the partly-filled d-electron shells are less shielded than, for example, the partly-filled f-electron shells or the rare earths. The d-electrons are profoundly influenced by the surrounding ligands and the effects of metal-ligand-metal bonding may be studied with greater ease.⁴

The simplest antiferromagnetic system consists of a pair of ions, each having an electron with a spin of 1/2. If the ions are close together one may expect an interaction of the exchange type between the nearest neighbors, and this interaction may be represented by the Hamiltonian, $-J \mathbf{S}_i \cdot \mathbf{S}_j$, where \mathbf{S}_i and \mathbf{S}_j are the Spin Quantum Number Operators for the electrons i and j , and J is the antiferromagnetic exchange coupling constant. A rough measure of the coupling constant can often indicate, for example, whether two nuclei are directly bonded or are separated by other atoms.

BACKGROUND AND THEORY

Although Porphyrin itself does not exist in nature, the porphyrin ring system is found in several very important natural products, notably haemoglobin, the cytochromes, catalase, peroxidase; chlorophyll and Vitamin B₁₂. Haemoglobin is present in the red blood corpuscles and functions to carry oxygen from the lungs to the body tissue. It consists of an iron-containing prosthetic group called Heme, which is bound to the protein globin. Acid hydrolysis of Haemoglobin liberates the prosthetic group as a complex ferric salt known as Hemin, Figure 1.

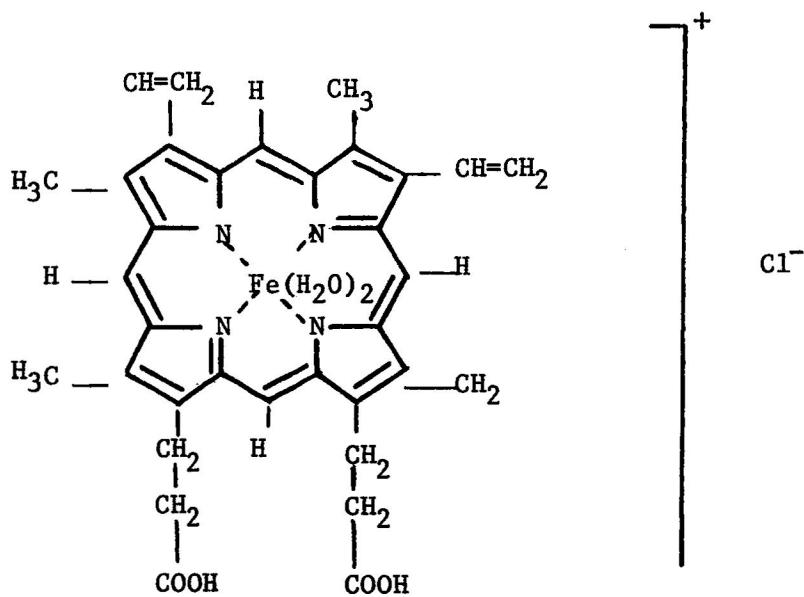
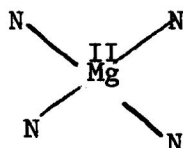
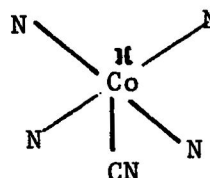


Figure 1. Hemin or Fe^{III} Protoporphyrin

This same heme group is the prosthetic group for the cytochromes, catalase and peroxidase. In chlorophyll the pyrrole nitrogens are complexed with Mg^{II} as



complexed with Co^{II} as



while in vitamin B_{12} , they are

The porphyrins are derived formally from porphin or porphine (Figure 2) by substitution of some or all of the hydrogen atoms 1 through 8 (fig. 2) with various side chains. Porphin has four meso positions

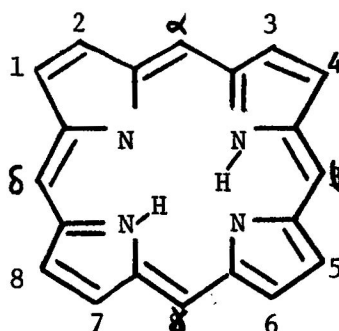


Figure 2. Porphin

(α through δ), more commonly known as methene bridge carbons, and substitution at these positions is not found to occur in nature. The porphyrin macrocycle is highly conjugated with eleven double bonds, and a number of resonance forms can be written. When coordination occurs the two protons are lost from the pyrrole nitrogens, leaving two negative charges which are perhaps distributed equally about the entire inner ring. The nucleus can also accept protons and behave as a basic centre. Overall, the porphyrin shows weak acidic properties, and the neutral species is stable

even in concentrated sodium hydroxide.⁵

The porphyrin nucleus is a tetradentate ligand in which the space available for a coordinated metal has a maximum diameter of $3.7\overset{\circ}{\text{\AA}}$. Metalloporphyrins form a set of compounds in which the metal may be four-coordinated with a square-planar geometry, five coordinated with a square pyramidal geometry, or six coordinated with a distorted octahedral geometry. Most form square planar complexes with the metal ion in the plane of the four pyrrole nitrogens, however, sometimes two of the pyrrole rings are tilted up and two are tilted down so that the nitrogen atoms are slightly out of plane. The porphyrin in the "free" environment probably exists in a near planar conformation with a low energy barrier relative to deviations from planarity. This condition makes for the conformational adaptability of the porphyrin skeleton to its surroundings. Because of the small amount of energy necessary to change its skeletal conformation, it is difficult in general to predict its structure under varying circumstances; that is, the detailed conformations of porphyrins in solutions are not known because solvent-porphyrin interactions are not well enough understood to know the detailed effects they might have on the easily deformed porphyrin skeleton.⁶ Thus, the porphyrin molecule is not completely rigid and its geometry can be influenced greatly by intramolecular interactions.

There is some degree of inability of the porphyrin ring system to adjust itself to fit a metal ion in the metalloporphyrin.⁷ Thus, there is an increase in the metal-nitrogen bond distance from $1.96\overset{\circ}{\text{\AA}}$ in nickel (II) porphyrins to $2.00\overset{\circ}{\text{\AA}}$ in palladium (II) porphyrins which is somewhat smaller than might be expected from the differences in their ionic radii of 0.72 and $0.86\overset{\circ}{\text{\AA}}$ respectively. Usually, the $\text{Fe}^{\text{III}}\text{-N}$ bond distance in

high spin Amines is 2.30 \AA , due largely to the antibonding d-electrons of the ferric ion. In ferric high spin pophyrins, however, the $\text{Fe}^{\text{III}}\text{-N}$ distance shrinks to 2.07 \AA due probably to the charge on the pyrolle nitrogens, but still too large to be accommodated in the plane of the nitrogens. (See Figure 5) .

A ferric porphyrin complex is called a Hematin when a hydroxy ion is coordinated with it, and a Hemin (Figure 3) when the coordinated anion is a halide or an acidic anion such as an acetate or a formate.

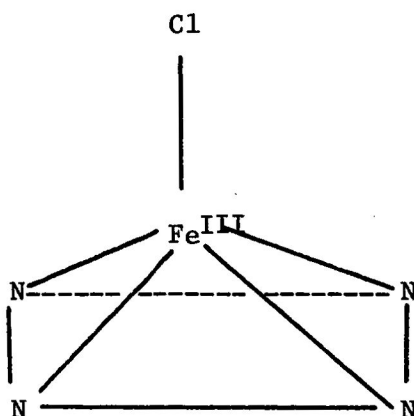


Figure 3. Hemin

If one adds ferric porphyrin to a solution of KOH, etc. , a new species results which has been characterized as μ -Oxo-bis (porphyrinatoiron (III)), dimer with the general structure as shown in Figure 4.

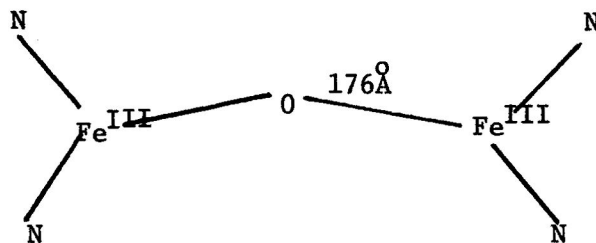


Figure 4. Structure of μ -Oxo-bis (porphyriniron (III)) dimer.

The iron in this five coordinated complex is 0.5 \AA out of the plane of the pyrrole nitrogens toward the oxygen bridge,⁸ (Figure 5).

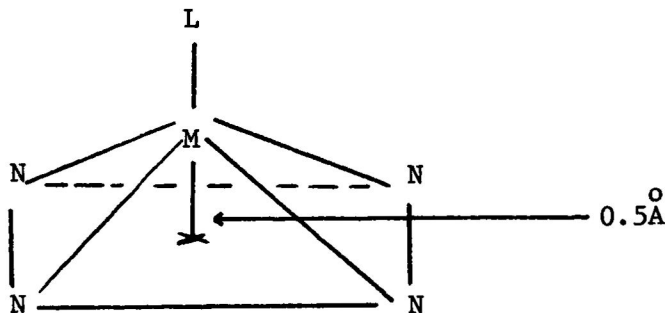


Figure 5.

The μ -Oxo-bis (tetraphenylporphyrinatoiron (III)) and the μ -oxo-bis (octaethylporphyrinatoiron (III)) dimers are synthetic porphyrins with phenyl groups at the methene bridge carbons and ethyl groups at the 1 thru 8 positions respectively. These bulky substituents, particularly the phenyl groups which are situated almost 90° out of the plane of the molecule, and the ethyl groups cause a tremendous amount of puckering in the molecule.

All known iron (III) porphyrins are paramagnetic, i.e., whether they are high spin, with the maximum number of unpaired electrons, or low spin, with the minimum number of unpaired electrons, they are attracted into a magnetic field. These substances have a resultant magnetic moment, the magnitude of which gives an accurate idea of the number of unpaired electrons they possess. A more useful parameter is the magnetic susceptibility which is heavily considered in the elucidation of electronic structures. Paramagnetic susceptibility depends inversely on temperature and often follows or approximates the behavior required by the Curie-Weiss

law
$$\chi_m^{\text{corr}} = \frac{C}{T + \theta}$$

where C = Curie constant,

θ = Weiss constant

χ_m^{corr} = magnetic susceptibility minus
diamagnetic susceptibility

Graphically, the above expression may be shown as Figure 6.

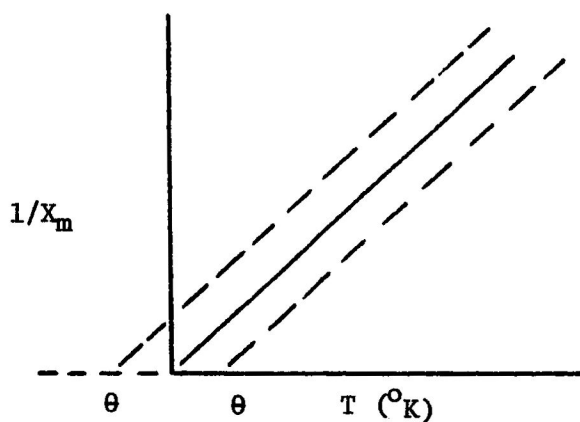


Figure 6.

The solid line represents the Curie formula $\chi_m^{\text{corr}} = \frac{C}{T}$ where C is the slope of the line. The dotted lines show experimental deviations from the Curie law, and θ , the Weiss constant, shows the temperature at which the line crosses the T axis. The Weiss constant takes into account both interionic and intermolecular interactions.⁹ If the magnetic susceptibility is measured at varying temperatures, a plot of χ_m^{corr} vs Temperature (absolute) results in the curve shown in Figure 7.

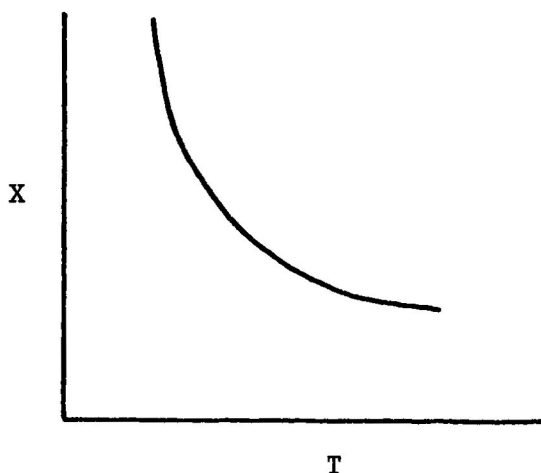


Figure 7. Plot of X vs T for Paramagnetic ion

This curve is typical of ions that are simple paramagnetics where the magnetic susceptibility decreases as the temperatures increases. Not all paramagnetic substances follow the simple case above however, and if the substance is a dimer, the paramagnetism has to be modified to account for an additional phenomenon.

A number of conditions are necessary in order that a system may have antiferromagnetic behaviour:

- a) whenever half-full orbitals of two magnetic cations overlap the two ends of a given anion p-orbital.
- b) whenever empty orbitals of two magnetic cations overlap the two ends of a given anion p-orbital.
- c) whenever an empty orbital of a magnetic cation overlaps one end of an anion p-orbital, and one half full orbital of another magnetic cation overlaps the other end of the same anion orbital.¹⁰

If two ions are close together, one may expect an interaction of the

exchange type. This exchange interaction may manifest itself in two forms viz:

- i) Direct exchange in which there is some interaction between the d-orbital on metal ion 1 with the d-orbital on metal ion 2. See Figure 8.

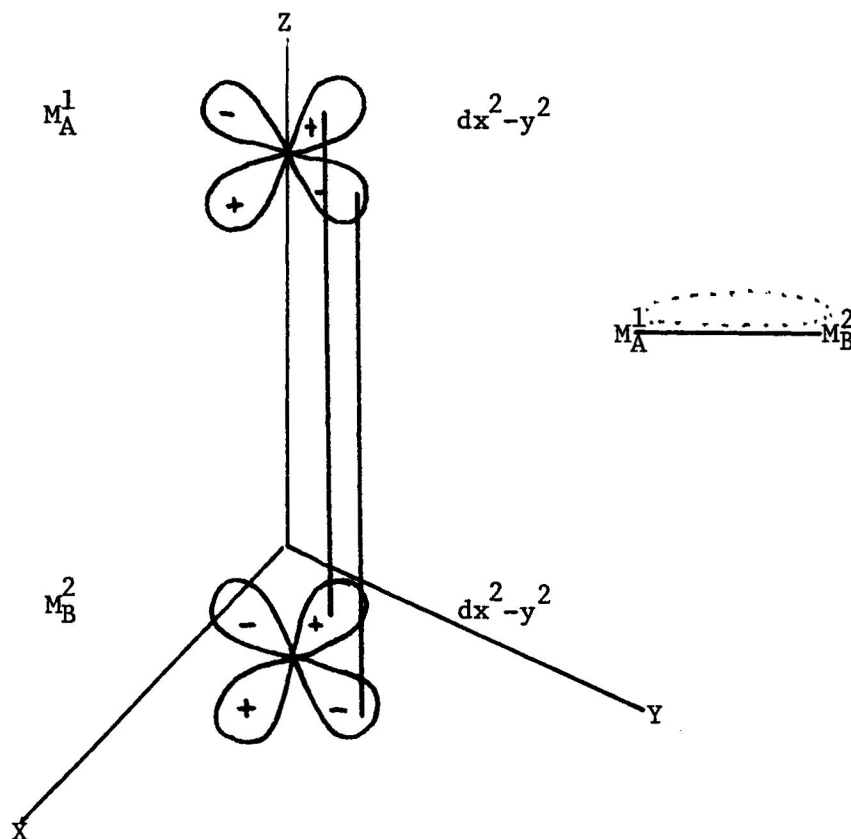


Figure 8. Overlap of d-orbitals

This mechanism involves direct overlap between the orbitals containing the unpaired electrons. For this model, the coupling constant J_{AB} is simply expressed by the exchange integral, as

$$J_{AB} = \int \phi_A(1) \phi_A(2) \frac{1}{r_{12}} \phi_B(2) \phi_B(1) d\tau$$

- ii) Superexchange where the exchange coupling between the ions is not due to direct overlap of their d-orbitals.¹¹ Instead, the spin is transmitted through the intervening ligand as shown in Figure 9.

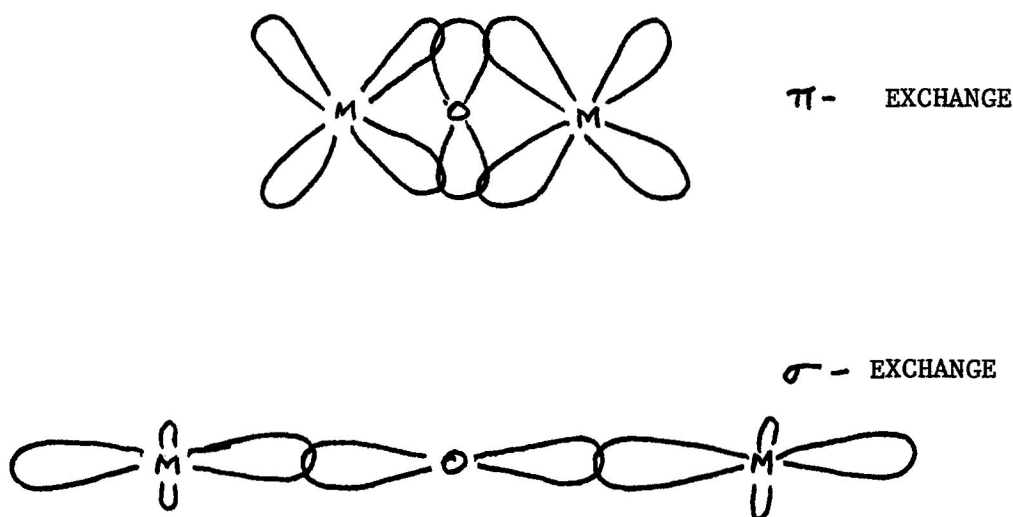


Figure 9. Exchange Coupling Across Oxygen Bridge

Superexchange best explains the antiferromagnetism of dimeric compounds in which the electric moments of the ions align themselves so as to cancel each other. The net result is that by the intervention of the oxygen atom, we obtain from a system in which the two metal ion d-electrons were free to orient their spins independently, one in which they are coupled together with their spins antiparallel. If this state is of lower energy than the uncoupled state, then as the temperature is lowered antiferromagnetism will be observed. As the temperature is raised, the efficiency of the interaction becomes less

pronounced and the susceptibility increases. Finally a critical temperature T_n (the Neel' Temperature) will be reached above which the spins are "free" and the antiferromagnetic material becomes paramagnetic.¹² Figure 10.

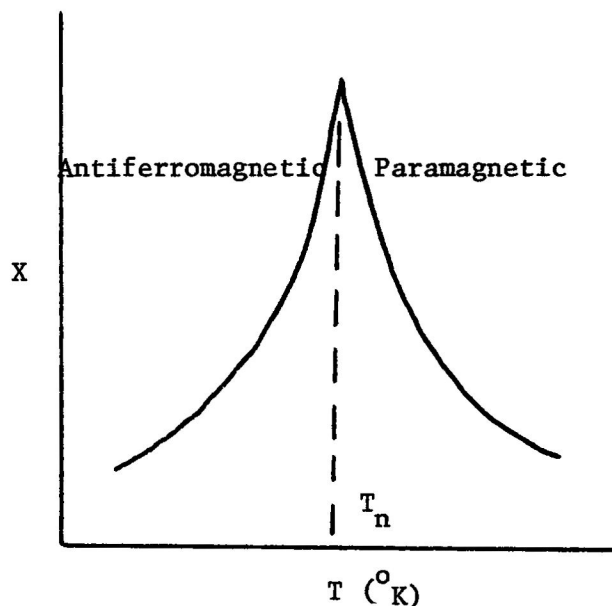


Figure 10. X vs T for antiferromagnetic compound

For systems that react antiferromagnetically the spin-only Hamiltonian, $-J \sum S_i \cdot S_j$ is used to evaluate the exchange coupling constant J. If J is positive, the system is Ferromagnetic, i.e., the spin moments are oriented parallel to each other. If, however, J is negative, the system is antiferromagnetic, i.e., an antiparallel alignment of spins.

The spin-only Hamiltonian is used for the evaluation of J because of the following qualitative argument:

For an electron in a particular orbital to have orbital angular

momentum about a chosen axis it must upon rotation about that axis transform the orbital into one which is equivalently degenerate.

In a "free ion" in which the five d-orbitals are degenerate, a rotation through 45° converts the d_{xy} into the $d_{x^2-y^2}$ orbital, and a rotation through 90° transforms the d_{xz} into d_{yz} . See Figure 11.

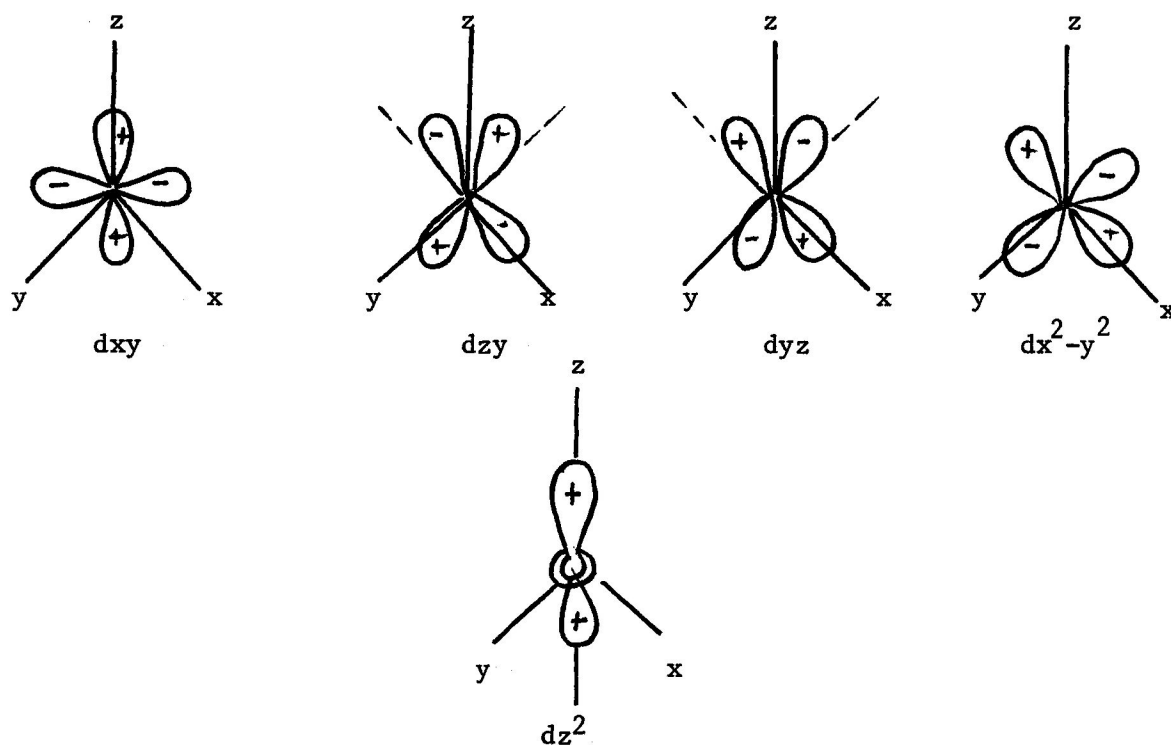
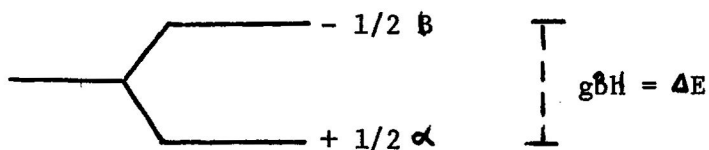


Figure 11. The d-orbitals

The d_z^2 cannot be transformed into any orbital by rotation about the z axis, and as a result, an electron in this orbital cannot give rise to any orbital contribution to the magnetic moment. During the formation of an octahedral complex, the incoming ligand splits the d-orbitals

into the t_{2g} (dxy, dyz, dxz) set, and the e_g (dz^2 , dx^2-y^2) set which are then separated by the ligand field splitting, $10 Dq$. As a consequence, the degeneracy of the dxy and dx^2-y^2 is destroyed and the orbital contribution from an electron in either of these orbitals is lost.¹³

In cases where molecules which can exist in different spin states are subjected to an external magnetic field, H , there is a Boltzmann distribution of the population of aligned dipoles between the energy levels. An example of this is the case of a species which contains one unpaired electron. The two spin states of the unpaired electron are unequal in energy in the presence of an external magnetic field, as shown below.



The distribution of particles with β spins and α spins is governed by the Boltzmann distribution law so that the ratio of

$$\frac{\beta \text{ spins}}{\alpha \text{ spins}} = e^{-\Delta E/kT}$$

where ΔE is the energy difference between states β and α and equals approximately 1 cm^{-1} under the influence of a magnetic field of 14000 gauss. kT is the thermal energy available to the system and $\approx 200 \text{ cm}^{-1}$ at 25° .

An atom or molecule when placed in a magnetic field acquires energy which may be expressed as a function of H . It may be written

as a series in H namely:

$$E_i = A_i + B_i H + C_i H^2 \dots$$

where A_i is the energy of the level in the absence of the field B_i and C_i are first and second order Zeeman coefficients.

The magnetic moment U_i is defined as

$$U_i = \frac{\partial E_i}{\partial H}$$

and when expressed as the average magnetic moment per gram ion the Boltzman expression becomes

$$M = N \frac{\sum_i U_i e^{-E_i/kT}}{\sum_i e^{-E_i/kT}}$$

Here, N is the number of atoms, usually taken as one mole of atoms.

Since $X = \frac{M}{H}$ = magnetic susceptibility

$$X = \frac{N}{H} \frac{\sum_i (-E_i / \partial H) e^{-E_i/kT}}{\sum_i e^{-E_i/kT}} \quad 1$$

We now need to determine E_i as a function of the applied magnetic field.

Recalling that $H = -J \sum_{ij} S_i S_j$ for a spin-only interaction, if we make the total spin $S' = S_i + S_j$, then the above is rewritten as

$$H = \frac{-2J}{n-1} \left\{ S' (S' + 1) - S_i (S_i + 1) - S_j (S_j + 1) \right\}_2$$

where Z = the number of nearest neighbours and

N = the number of paramagnetic ions in the molecule contributing

to the interaction.

The constant terms may be ignored since the energy under consideration is relative. Hence, equation 2 can be rewritten as $H = \frac{-J}{2} S'(S'+1)$. Combining the applied magnetic field contribution taken parallel to the z axis gives the expression:

$$H = \frac{-ZJ}{2} S'(S'+1) + gBHS'_z$$

where g is the Lande splitting factor and B is the Bohr magneton. If

we write a set of basic wavefunctions as $|S'M'S\rangle$ then $H|S'M'S\rangle = \left\{ \left(\frac{-ZJ}{2} S'(S'+1) + gBHM'S \right) \right\} |S'M'S\rangle$ where $|S'M'S\rangle$ are eigen functions

and $\frac{-ZJ}{2} S'(S'+1) + gBHM'S$ are eigen values.¹⁴

Consider as an illustration the case where $S_1 = S_2 = 1/2$, i.e. 1 unpaired electron $S' = 1, 0$.

$$M'S = S_1 + S_2, S_1 + S_2 - 1, S_1 + S_2 - 2, S_1 - S_2$$

$$= \quad 1 \quad \quad 0 \quad \quad -1 \quad \quad 0$$

$$S' \quad M'S \quad \quad \frac{-J}{2} S'(S'+1) + gBHM'S$$

$$1 \quad 1 \quad \quad \frac{-J}{2} \times 2 + gBH = -J + gBH$$

$$1 \quad 0 \quad \quad \frac{-J}{2} \times 2 + 0 = -J$$

$$1 \quad -1 \quad \quad \frac{-J}{2} \times 2 + (-gBH) = -J - gBH$$

$$0 \quad 0 \quad \quad 0 \quad \quad 0$$

$$-J + gBH$$

$$-J \quad \text{are } E_i \text{ values which are required}$$

$$-J - gBH$$

to calculate the magnetic susceptibility of the species. From equation

1 we take the partial derivatives of the E_i values with respect to H which result as follows:

$$\frac{\partial E_i}{\partial H} (-J + gBH) = gB$$

$$\frac{\partial E_i}{\partial H} (-J) = 0$$

$$\frac{\partial E_i}{\partial H} (-J - gBH) = -gB$$

substituting in equation 1 we have:

$$X_z = \frac{1}{2} \frac{N}{H} \frac{(-gB e^{J-gBH/kT} + gB e^{J+gBH/kT})}{(e^{J-gBH/kT} + e^{J/kT} + e^{J+gBH/kT} + e^0 = 1.)} \quad (3)$$

Reducing equation 3

$$\begin{aligned} \text{a) } & -gBe^{J/kT} (1-gBH/kT) + gBe^{J/kT} (gBH/kT + 1) \quad (\text{numerator}) \\ & = 2g^2 B^2 H/kT e^{J/kT} \end{aligned}$$

$$\begin{aligned} \text{b) } & e^{J/kT} (1-gBH/kT) + e^{J/kT} + e^{J/kT} (1+gBH/kT) + 1 \quad (\text{denominator}) \\ & = 3e^{J/kT} \end{aligned}$$

Combining a and b

$$X_z = \frac{1}{2} \frac{N}{H} \frac{2g^2 B^2 H / kT e^{J/kT}}{3e^{J/kT} + 1}$$

$$\text{giving finally } X_z = \frac{Ng^2 B^2 e^{J/kT}}{kT (3e^{J/kT} + 1)} \quad (4)$$

Equation 4 is of the form $y = ae^{bx}$ and so a non-linear least squares computer program (written by Dr. G. S. Owen)¹⁵ was used to evaluate J as a function of X and T . These programs were written for ions having spins of $5/2$, $5/2$ and $5/2$, $4/2$.

EXPERIMENTAL

Electrolytic oxidation consists of applying a constant potential to remove an electron from each of the prepared μ -oxo-dimers. The first oxidation potential of $(\text{FeTPP})_2\text{O}$ was found to be 1.15 volts, and that of $(\text{FeOEP})_2\text{O}$ 0.98 volts.

Apparatus. The electrolysis apparatus consisted of the following: a D.C. power supply, milliammeter (custom built by G. O'Brien of Georgia Institute of Technology), high impedance voltmeter, and a reaction vessel (custom built by Don Lilly of Georgia Institute of Technology).

The set up for an experiment is shown in Figure 12. Prior to an experiment the reaction vessel was washed with water, ethanol and CH_2Cl_2 , and dried overnight in an oven at 60° . A solution of 0.1 M. TPAP in CH_2Cl_2 was poured into the reaction vessel-enough to cover the platinum gauze. Argon gas was bubbled in the reaction vessel throughout the experiment. The solution was stirred by a magnetic stirring bar. A potential of 1.5 volts was applied to remove oxidizable materials from the solution¹⁶ before introduction of the μ -oxo-dimer. Dry porphyrin was then added to the solution to reach the desired concentration. Care should be taken not to have the solution too concentrated as this seems to increase the resistance considerably and inhibit the progress of the reaction at the expected potential. The controlled potential lead was then connected and the voltmeter set at the desired potential. As the electrons leave the solution, the

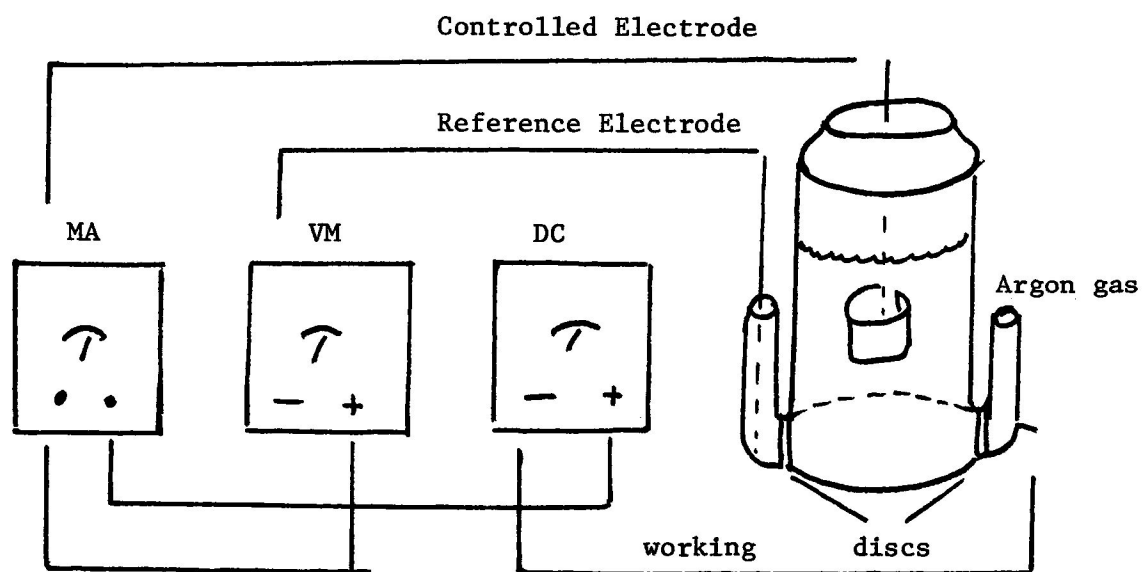


Figure 12. Electrolysis Apparatus.

potential across the control and reference leads was increased. This increase was most noticeable at the start of the oxidation process, and so the potential must be watched and controlled at a constant value. As the number of oxidizable ions decrease, the increase in the potential became less noticeable, and the D.C. current approached zero. The oxidized material was removed from the reaction vessel and placed on a rotary evaporator to remove the CH_2Cl_2 . The residue was washed with hot water and filtered to remove TPAP, then washed with Benzene to remove the neutral parent compound, thus leaving the oxidized species in crystalline form. The oxidized porphyrins were isolated as the perchlorate salts (ClO_4^-) ,¹⁷ and then kept in vacuum. Before further experiments were attempted, they were washed with benzene and dried, since they decay at the rate of a few percent per day.

Optical spectra were taken before, during, and after the experiment on a Cary 17 Spectrophotometer. This was used to monitor the extent of the oxidation. These spectra of both the neutral and oxidized species show an almost complete disappearance of the product peaks at 570 nm and 610 nm; reduction in the absorbance of the 406 nm Soret band, and a slight shift towards high wavelength. (See Figure 13). In the $(\text{FeOEP})_2\text{O}$, the Soret band is at 385 nm and the oxidized species at 380 nm. (See Figures 13 and 14). The following extinction coefficients were calculated from spectra taken. (See Table 1)

TABLE 1. Extinction Coefficients for $(\text{FeTPP})_2\text{O}$, $(\text{FeTPP})_2\text{O}^+$, $(\text{FeOEP})_2\text{O}$ and $(\text{FeOEP})_2\text{O}^+$

$(\text{FeTPP})_2\text{O}$	λ nm	ϵ		$(\text{FeTPP})_2\text{O}^+$	λ nm	ϵ	
	406	107.0	$\times 10^3$		406	84.6	$\times 10^3$
	570	8.7	$\times 10^3$		570	6.8	$\times 10^3$
	610	4.04	$\times 10^3$		650	2.65	$\times 10^3$
	650	.05	$\times 10^3$				
$(\text{FeOEP})_2\text{O}$	385	63.0	$\times 10^3$	$(\text{FeOEP})_2\text{O}^+$	380	51.0	$\times 10^3$
	620	1.745	$\times 10^3$		500	5.14	$\times 10^3$

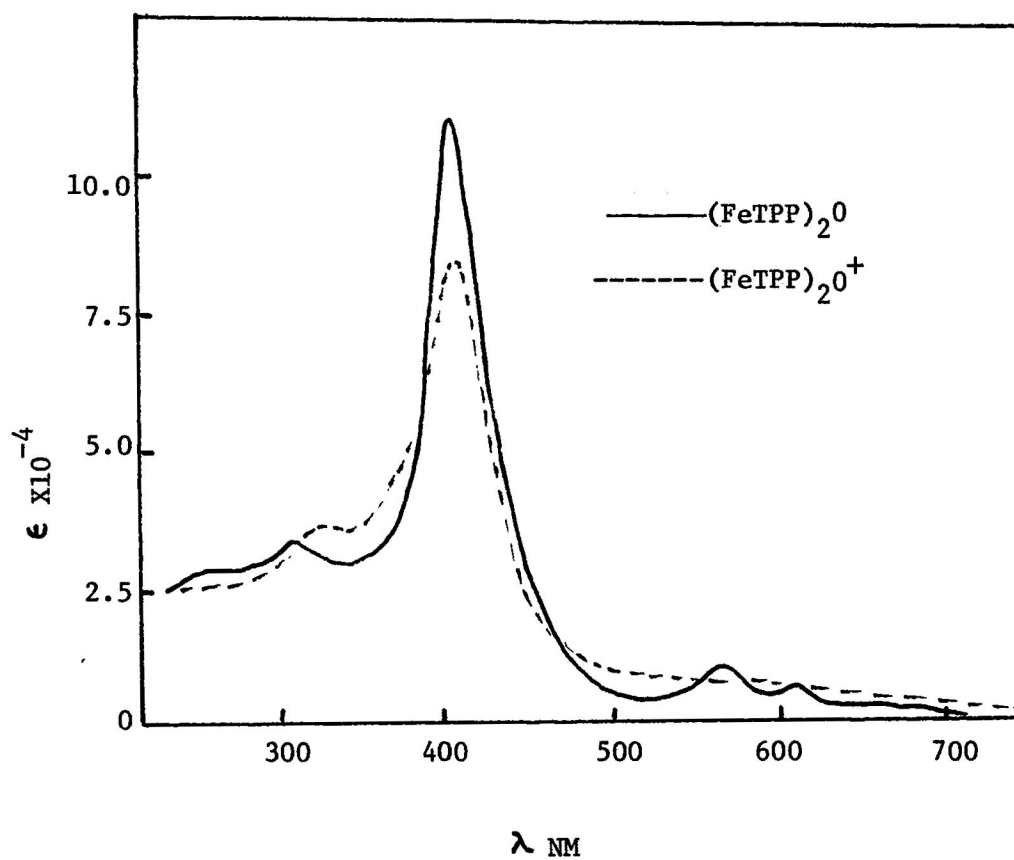


Figure 13. Optical Spectrum of Neutral and Oxidized Porphyrins.

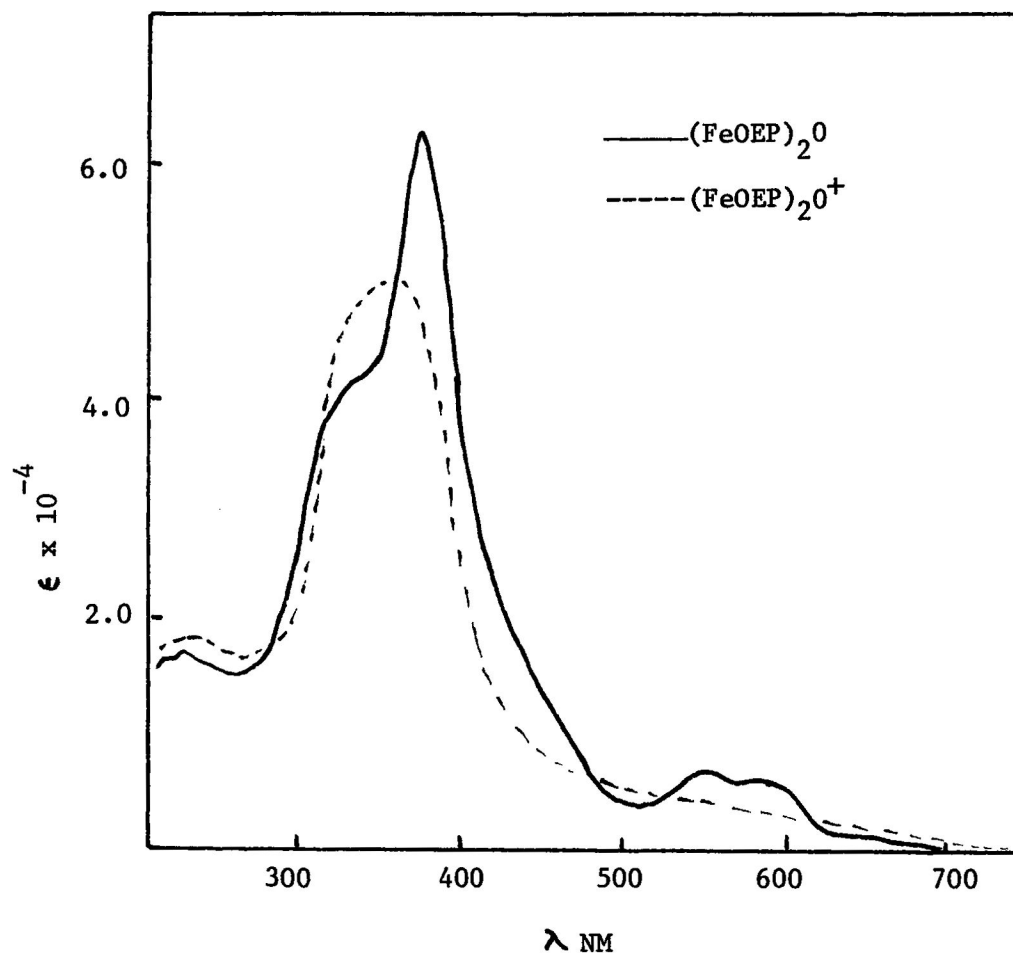


Figure 14. Optical Spectrum of Neutral and Oxidized Porphyrins.

Dichloromethane was distilled from calcium hydride, collected and stored over molecular sieves (Linde, No. 4A). Tetrapropyl ammonium perchlorate (TPAP) was recrystallized from 95% ethanol and stored in a vacuum oven at room temperature.¹⁸

μ-Oxo-bis (tetraphenylporphyrinatoiron (III)), (FeTPP)₂O, was prepared from tetraphenylporphyrinatoiron (III) chloride (FeTPPCl). Approximately 1 gram of FeTPPCl was dissolved in 400 ml CH₂Cl₂ and an equal amount of 10% KOH added. After stirring the solution for an hour the KOH portion was withdrawn using a separatory funnel. The remaining solution, (FeTPP)₂O in CH₂Cl₂, was washed 5 times with distilled water to remove traces of KOH, then dried for about 12 hours over K₂CO₃ to remove aqueous residues. The (FeTPP)₂O was recrystallized in approximately 200 ml of CH₂Cl₂ and an equal volume of Hexane. The solution was placed in the fume hood to allow for the evaporation of the volatile solvents. The (FeTPP)₂O was placed in a vacuum oven, and residual traces of the solvent were removed with pumping. *μ*-Oxo-bis (octaethylporphyrinatoiron (III)) (FeOEP)₂O, was prepared from octaethylporphyrinatoiron (III) chloride (FeOEPCL). Its preparation and recrystallization were identical to that of the (FeTPP)₂O as described above. (FeOEP)₂O was dried over Na₂SO₄. Both crystalline *μ*-oxo-dimers were washed with hexane to remove unreacted chlorides and other impurities. They were kept in vacuum and vented to argon before use.

Nuclear magnetic resonance (nmr) experiments were done, using a Varian A-60A NMR Spectrometer with a variable temperature apparatus with both the neutral and the oxidized species of the porphyrin *μ*-oxo-dimers. The samples were prepared with CH₂Cl₂ as solvent at concentrations of

$\approx 10^{-3}$ g/ml. Special concentric nmr (Wilmad #517) tubes were used with the solvent in the smaller inner tube and the sample + solvent in the larger outer tube. Before an experiment was performed the variable temperature apparatus was calibrated with a methanol sample at -60° and $+40^{\circ}$. Shifts in the nmr methanol peaks should correspond closely with values in the nmr manual. Each sample was run at various temperatures, and splittings on the CH_2Cl_2 peak were observed. These splittings, ΔF , measured in H_z , were used to evaluate the magnetic susceptibilities of the species Figure 15. The relationship used for the calculation of the magnetic susceptibility is as follows:¹⁹

$$X = \frac{3 \Delta F}{2 \pi F m} + X_0 + \frac{X_0 (d_0 - d_s)}{m} + X_{\text{H}_2\text{TPP}}$$

where X = magnetic susceptibility of the dissolved substance per gram

ΔF = frequency of separation splitting on solvent peak in H_z

F = frequency of the nmr in H_z

m = mass of solute in g/ml

X_0 = diamagnetic susceptibility of the solvent

d_0, d_s = densities of solvent and solute respectively

($d_0 - d_s$) was taken to be equal to $-m$).

$X_{\text{H}_2\text{TPP}}$ = diamagnetic susceptibility of porphyrin.

As the temperature varies a density correction expressed is applied to the solvent²⁰ which subsequently causes a change in the mass of the solute viz:

$$M^{\text{corr}} = M \left(1 + \frac{\Delta \rho}{\rho} \right) \text{ where } \frac{\Delta \rho}{\rho} \text{ is computed graphically}$$

over the temperature range. (See Figure 16). A typical calculation

using $(\text{FeOEP})_2$ at room temperature shows the following results.

$$A_{620} = 0.9$$

$$\epsilon_{620} = 1745$$

$$C = 5.4 \times 10^{-3} \text{ (from Beers law)}$$

$$M_{\text{corr}} = 3.3 \times 10^{-3}$$

$$X^C = \frac{7.96 \times 10^{-9} \times 1.75}{3.3 \times 10^{-3}} - \frac{0.53 \times 10^{-6}}{}$$

$$= 3.69 \times 10^{-6} \text{ where } 1.75 \text{ is } \Delta F.$$

From the magnetic susceptibility the magnetic moment per ion is computed using the expression:

$$U = 2.84 (X \cdot \text{Mwt} \cdot T)^{\frac{1}{2}} = 2.84 (3.69 \times 10^{-6} \cdot 604 \cdot 300)^{\frac{1}{2}}$$

$$= 2.30 \text{ Bohr magneton.}$$

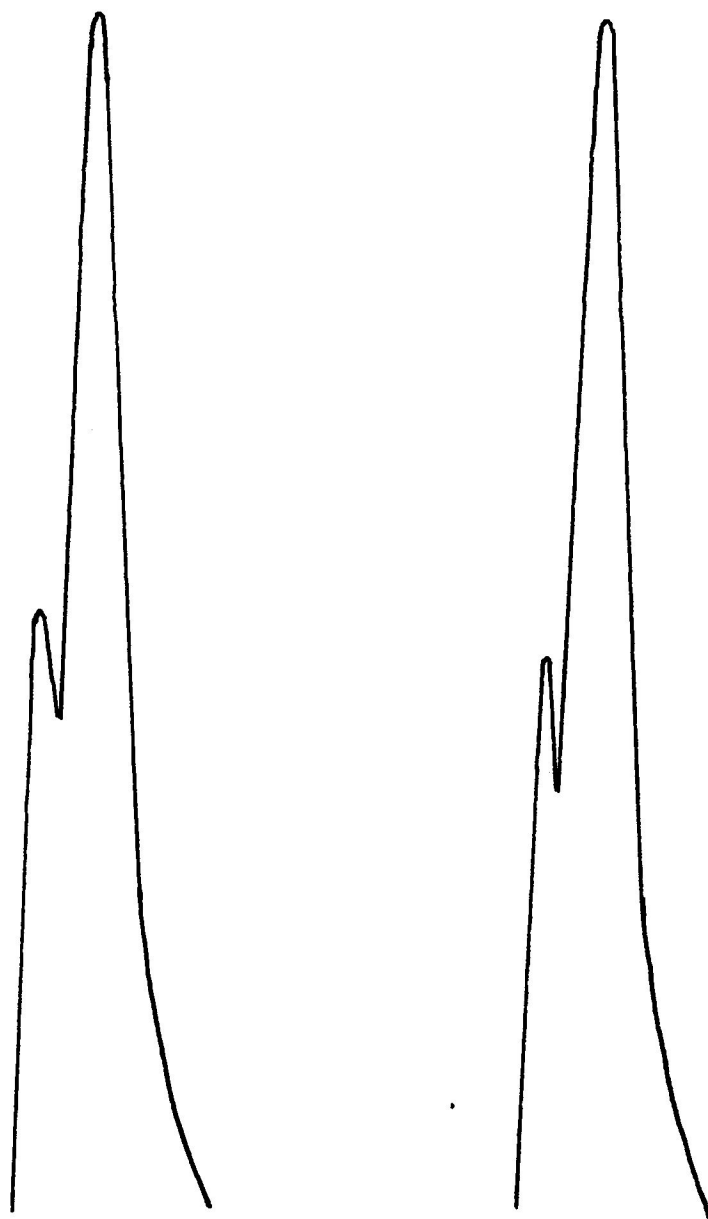


Figure 15.

NMR Spectrum of CH_2Cl_2 Showing Splitting ΔF .

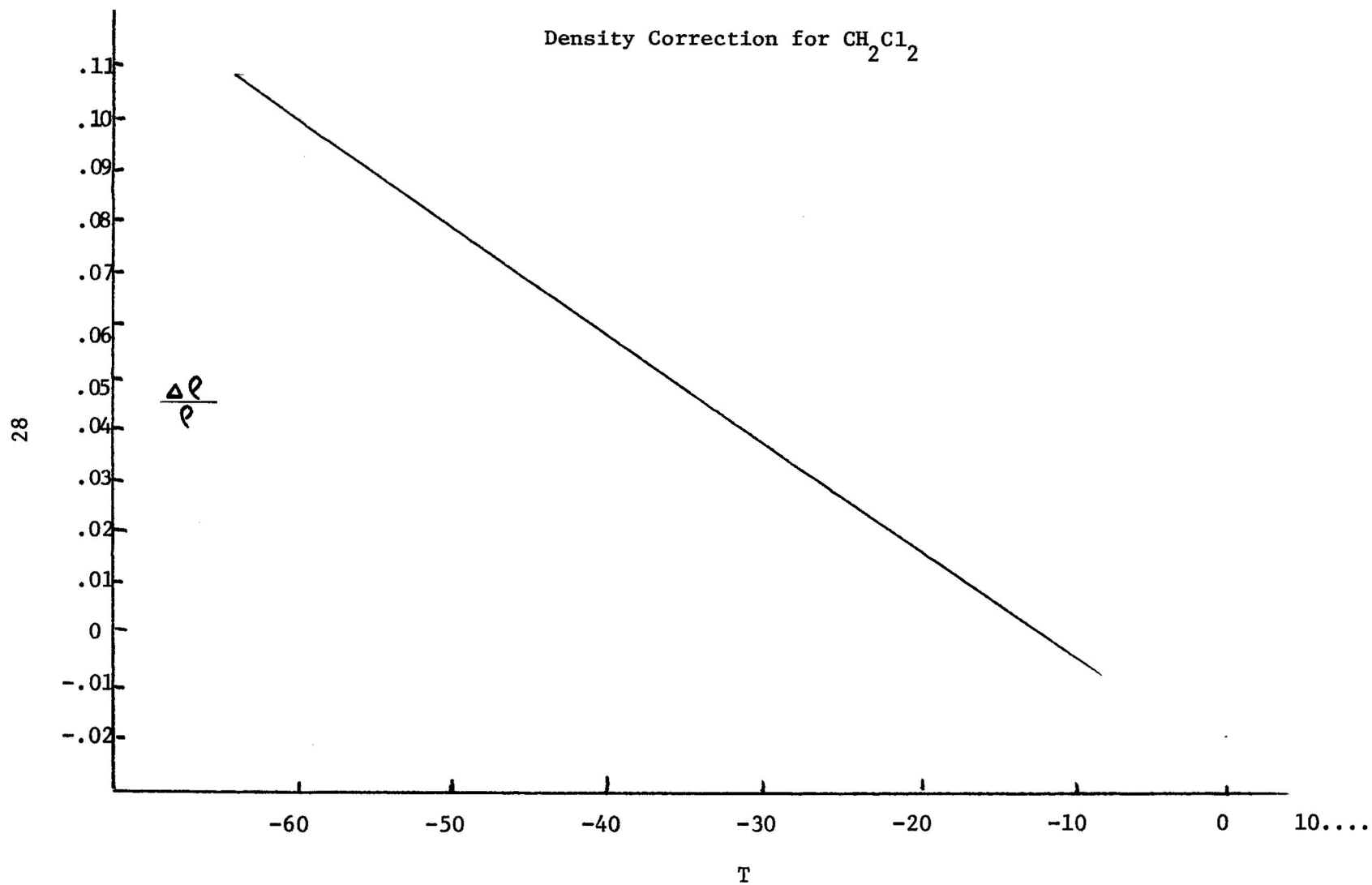


Figure 16.
Density Correction Graph

RESULTS AND DISCUSSION

Experimental data along with the results obtained are tabulated in Tables 3 through 7. The average J values are shown in Table 6.

The absolute values of J give some indication of the behavior of the Fe-O-Fe system. J is proportional to the electron density in both the metal and the oxygen orbitals; to the Fe-O orbital overlap and thus, the Fe-O bond distance.

For the neutral species:

$$\left| J(\text{FeTPP})_2\text{O} \right| = 344 \text{ cm}^{-1} \pm 40 \gg \left| J(\text{FeOEP})_2\text{O} \right| = 280 \text{ cm}^{-1} \pm 34$$

For the oxidized species:

$$\left| J(\text{FeTPP})_2\text{O}^+ \right| = 154 \text{ cm}^{-1} \pm 42 \gg \left| J(\text{FeOEP})_2\text{O}^+ \right| = 73 \text{ cm}^{-1} \pm 1$$

These results clearly show strong antiferromagnetic interaction both for the neutral and the oxidized species. However, it must be considered that the differences in the values of the TPP and OEP are due to effects of substituents on the ring. In the TPP the phenyl groups are tilted out of the plane of the ring, and they possess, though not strongly, electron donating ability. Indeed, since the porphyrin molecule is not a completely rigid system, the phenyl groups in solution can readily assume varying orientations with respect to the rest of the molecule. Thus, some π -electron donation can be expected from the phenyl groups, increasing the density in the Fe orbitals.

The OEP on the other hand has its ethyl groups in the plane of the ring but they are weakly electron donating. Additional evidence of

π -electron donation from the phenyl rings can be drawn from the fact that the optical spectrum of the $(\text{FeTPP})_2\text{O}$, is red shifted compared to the $(\text{FeOEP})_2\text{O}$ (see below), and so, greater electron delocalization is expected.

	λ_{max}			
$(\text{FeTPP})_2\text{O}$	610	570	405	(Soret)
$(\text{FeOEP})_2\text{O}$	585	555	390	(Soret)

Further, knight shift measurements of $(\text{FeTPP})_2\text{O}$, and $(\text{FeOEP})_2\text{O}$ give the following results:²¹

TABLE 2

KNIGHT SHIFT MEASUREMENTS OF PYRROLE PROTONS

		B	M	O.P
S = 0	ZnTPP	9.0	8.25	7.83
S = 1/2	$(\text{FeOEP})_2\text{O}$	6.1	5.2	1.8
S = 1/2	$(\text{FeTPP})_2\text{O}$	13.6	7.6	7.6

Here the measurements are taken relative to ZnTPP which is a diamagnetic species. The values for the TPP are higher than for the OEP, thus suggesting greater electron delocalization by the TPP.

This increase in the electron density of the Fe orbitals of the $(\text{FeTPP})_2\text{O}$, as opposed to the $(\text{FeOEP})_2\text{O}$, explains the larger value of J in the $(\text{FeTPP})_2\text{O}$ system. The first oxidation products result in smaller J values than the neutral species. Here, the electron density is removed from the Fe orbitals as the system goes from Fe^{III} to Fe^{IV} . Thus, the electron density in the Fe orbitals

is lowered. As previously mentioned, the Fe^{III} ion is 0.5 \AA out of the plane of the pyrrole nitrogens. This decrease in electron density results in a decrease in the effective size of the Fe ion thus enabling it to move closer into the plane of the molecule. This allows for an increase in the $\text{Fe}^{\text{IV}}-\text{O}$ bond length. Thus, the overlap between the Fe and O orbitals is decreased. These two effects, lowering of electron density and of orbital overlap explain the decrease in J noted for the oxidized species.

TABLE 3

EXPERIMENTAL RESULTS FOR $(\text{FeTPP})_2\text{O}$

Concn m/l	M^{corr} g/ml	ΔF	Temp $^{\circ}\text{K}$	X^c	u.BM	J
2.41×10^{-3}	1.63×10^{-3}	0.6	296	2.40×10^{-6}	1.96	-346.92
	1.66	0.5	281	1.86	1.70	
	1.69	0.5	266	1.82	1.62	
	1.76	0.5	235	1.73	1.49	
	1.80	0.48	217	1.59	1.37	
3.07×10^{-3}	2.08	0.55	294	1.57	1.58	-396.62
	2.13	0.52	274	1.41	1.44	
	2.19	0.50	254	1.28	1.32	
	2.23	0.48	239	1.18	1.23	
	2.29	0.70	220	1.90	1.50	
5.23×10^{-3}	3.50	1.4	303	2.65	2.09	-259.8
	3.60	1.3	283	2.33	1.90	
	3.71	1.5	259	2.68	1.94	
	3.86	1.6	240	2.77	1.89	
	3.88	1.9	225	3.36	1.95	
	3.97	2.0	208	3.4	1.96	
4.79×10^{-3}	3.17×10^{-3}	0.9	320	1.72	1.73	-329.33
	3.23	0.9	300	1.68	1.64	
	3.34	1.2	273	2.32	1.85	
	3.43	1.3	253	2.48	1.84	
	3.52	1.3	233	2.40	1.74	
	3.63	1.05	213	1.77	1.43	

TABLE 3 -- Continued

Concn m/l	M ^{corr} g/ml	ΔF	Temp °K	X ^c	u.BM	J
3.44 x 10 ⁻³	2.33 x 10 ⁻³	0.65	298	1.68 x 10 ⁻⁶	1.65	-386.96
	2.36	0.65	285	1.65	1.60	
	2.45	0.70	258	1.74	1.56	
	2.47	0.57	247	1.53	1.43	
	2.60	0.55	210	1.15	1.14	

TABLE 4

EXPERIMENTAL RESULTS FOR $(\text{FeTPP})_2\text{O}^+$

Concn m/l	$M^{\text{corr}} \text{ g/ml} \times 10^{-3}$	ΔF	Temp $^{\circ}\text{K}$	$X^C \times 10^{-6}$	u.BM	J
$.84 \times 10^{-3}$.558	0.7	315	9.44	4.02	-121.45
	.572	0.76	294	10.04	4.01	
	.590	0.68	274	8.64	3.57	
	.606	0.70	254	8.66	3.46	
	.621	0.70	239	8.44	3.31	
	.632	0.40	220	4.50	2.32	
4.0×10^{-3}	2.60	3.25	308	9.42	3.97	-101.56
	2.70	3.20	293	9.02	3.78	
	2.98	3.30	273	8.61	3.58	
	2.86	3.02	253	7.87	3.28	
	2.93	4.3	233	11.15	3.75	
	3.0	5.4	213	13.79	3.99	
$.967 \times 10^{-3}$.965	0.9	313	6.89	3.43	-214.29
	.967	0.7	294	5.23	2.89	
	.992	0.6	277	4.28	2.54	
	1.017	0.5	260	3.38	2.18	
	1.05	0.55	233	3.64	2.14	
	1.205	0.8	312	6.15	2.84	
1.66×10^{-3}	1.23	0.9	293	6.74	3.28	-177.20
	1.27	0.85	273	6.10	3.02	
	1.30	0.80	253	5.65	2.79	
	1.30	0.70	228	4.72	2.42	
	1.38	0.70	206	4.58	2.26	

TABLE 5

EXPERIMENTAL RESULTS FOR $(\text{FeOEP})_2\text{O}$

Concn	$M^{\text{corr}}_{\text{g/ml}} \times 10^{-3}$	ΔF	Temp $^{\circ}\text{K}$	$X^c \times 10^{-6}$	u.BM	J
4.84×10^{-3}	4.84×10^{-3}	1.45	298	1.85	1.64	-314
	4.91	1.7	285	2.22	1.76	
	5.09	1.7	258	2.12	1.63	
	5.14	1.9	247	2.41	1.70	
	5.24	1.8	230	2.20	1.57	
	5.39	1.9	210	2.27	1.53	
2.25×10^{-3}	1.34×10^{-3}	0.45	306	2.13×10^{-6}	1.78	-246
	1.37	0.50	288	2.36	1.82	
	1.40	0.50	272	2.29	1.74	
	1.46	0.70	246	3.28	1.98	
	1.49	0.90	226	4.25	2.16	
	1.54	0.95	203	4.38	2.08	

TABLE 6
EXPERIMENTAL RESULTS FOR $(\text{FeOEP})_2^{0+}$

Concn	$M^{\text{corr}} \text{ g/ml} \times 10^{-3}$	ΔF	Temp $^{\circ}\text{K}$	$X^c \times 10^{-6}$	u.BM	J
3.48×10^{-3}	2.02	3.2	323	12.07	4.36	-72.56
	2.08	3.4	302	12.48	4.28	
	2.16	4.0	276	14.21	4.36	
	2.22	3.95	256	13.63	4.12	
	2.28	4.07	235	13.67	3.95	
	2.32	4.8	223	15.93	4.16	
2.25×10^{-3}	1.3	2.0	318	11.71	4.26	-73.36
	1.36	2.2	296	12.34	4.22	
	1.40	2.68	373	14.70	4.42	
	1.44	2.4	256	12.73	3.98	
	1.47	2.75	236	14.36	4.06	
	1.50	3.0	219	15.39	4.05	

TABLE 7

SUMMARIZED RESULTS FOR NEUTRAL AND
OXIDIZED TPP AND OEP

Compound	J
$(\text{FeTPP})_2\text{O}$	$344\text{cm}^{-1} \pm 40$
$(\text{FeTPP})_2\text{O}^+$	$-154\text{cm}^{-1} \pm 42$
$(\text{FeOEP})_2\text{O}$	$-280\text{cm}^{-1} \pm 34$
$(\text{FeOEP})_2\text{O}^+$	$-73\text{cm}^{-1} \pm 1$

Comparison of $(\text{FeTPP})_2\text{O}$ with published results $(\text{FeTPP})_2\text{O}$ (From Knight shift measurements of pyrrole protons)

$$253-325 \quad H = \frac{A H S_z}{g n^B m} \quad 22$$

$$(\text{FeTPP})_2\text{O} \quad A = 1.29 \times 10^5 H_z \quad J = -309 \text{ cm}^{-1} \pm 50 \text{ cm}^{-1}$$

$$(\text{FeT}_{\text{p}}\text{mPP})_2\text{O} \quad A = 1.44 \times 10^5 H_z \quad J = -335 \text{ cm}^{-1}$$

$$(\text{FeTPP})_2\text{O} \quad (\text{Fe-O-Fe} = 168^\circ) \quad J = -310 \text{ cm}^{-1}$$

$$(\text{FeTPP})_2\text{O} \quad \text{Solid State} \quad J = -380 \text{ cm}^{-1}$$

$$(\text{Fe}(\text{Salen}))_2\text{O} \quad (\text{Fe-O-Fe} = 142^\circ) \quad J = -174 \text{ cm}^{-1}$$

Done with non-porphyrin complexes $J = -170$ to -210 cm^{-1} Salen = N.M^1 -ethylene-bis (sulicylideneimine) (Tetradentate ligand)

$$H = -ZJ S_1, S_2 \quad J = \frac{1}{2} \text{ above values}$$

BIBLIOGRAPHY

1. P.O.W. Boyd and T. D. Smith, Inorg. Chem., 10, 2041 (1971).
2. R. H. Felton, G. S. Owen, J. Am. Chem. Soc., 93, 6332 (1971).
3. R. H. Felton, G. S. Owen, Annals of The New York Academy of Sciences 206, 210 (1973).
4. E. Konig, "Physical Methods in Advanced Inorganic Chemistry," Interscience, New York, 1968, p. 266.
5. J. E. Falk, "Porphyrins and Metalloporphyrins," Elsevier Pub. Co., New York, 1964, p. 27.
6. E. B. Fleischer, Accts. Chem. Res. 3, 105 (1970).
7. N. M. Hughes, "The Inorganic Chemistry of Biological Processes," John Wiley & Sons, London, 1974, p. 162.
8. E. B. Fleischer, J. Am. Chem. Soc., 93 3162 (1971).
9. F. A. Cotton and G. Wilkinson, "Advanced Inorganic Chemistry," Interscience, New York, 1966, p. 641.
10. D. E. G. Williams, "The Magnetic Properties of Matter," American Elsevier Pub. Co., Inc., New York, 1966, p. 191.
11. F. E. Mabbs and D. J. Machin, "Magnetism and Transition Metal Complexes," Chapman & Hall, London, 1973, p. 172.
12. J. G. Kirkwood and F. H. Westnemer, J. Chem. Phys., 6, 506 (1958).
13. K. Burger, I. T. Millar and D. W. Allen, "Coordination Chemistry: Experimental Methods," International Sci. Series England, 1973, p. 222.
14. R. M. Golding, "Applied Wave Mechanics," D. Van Nostrand Co., Ltd. London, 1969, p. 228.
16. J. Fajer, D. C. Borg, A. Forman, D. Dolphin, R. S. Felton, J. Amer. Chem. Soc., 92, 3451 (1970).
17. L. F. Feiser and M. Feiser, "Reagents for Organic Synthesis", Vol. 1, John Wiley and Sons, New York 1967, p. 191.

18. R. S. Felton, G. S. Owen, D. Dolphin, J. Fajer, J. Amer. Chem. Soc. 93, 6332 (1971).
19. D. F. Evans, J. Chem. Soc., 2003 (1959).
21. G. S. Owen, unpublished results.
22. T. Boyd and H. Smith, Inorg. Chem. 10, 9, 2041 (1971).